Simulation Study of a Small Water Cherenkov Detector: Investigating Neutron Backgrounds in Supernova Neutrino Detection

Bilguun Batbayar, University of Chicago
Yokoyama-Nakajima Group, Department of Physics, The University of Tokyo, Summer 2024

Abstract

The Spallation Neutron Source (SNS) at Oak Ridge National Laboratory (ORNL) is developing detectors designed to detect supernova neutrinos that effectively mitigates neutron backgrounds that interfere with true neutrino signals. This paper presents a proposed small water Cherenkov detector, employing Geant4 simulations to obtain relevant data and insights. The primary objective is to assess the effectiveness of common shielding materials, such as water and polyethylene, by constructing a barrier around the detector and determining the optimal thickness required to shield against neutron backgrounds. Additionally, optical simulations were conducted, and an attempt was made to reconstruct the neutron energy signal from photon hits recorded by photomultiplier tubes. A thorough understanding of the properties of neutrons produced within the detector is crucial for distinguishing them from other interaction products and reducing backgrounds. Moreover, designing future water Cherenkov detectors with shielding materials to minimize unwanted neutron signals will significantly enhance their response to supernova neutrino bursts.

I. INTRODUCTION

A. Water Cherenkov Detectors

A water Cherenkov detector detects Cherenkov radiation emitted from high-energy charged particles produced when neutrinos interact with water. When these charged particles exceed the speed of light in water, they generate Cherenkov photons. This emitted light is captured by photomultiplier tubes in the detector, which convert it into electrical signals for analysis. The collected data is then interpreted to identify neutrino events, including those from supernovae. In essence, these detectors are sensitive to charged particles generated by core-collapse supernova neutrinos in the few to tens of MeV range.

B. Supernova Neutrino Detection at ORNL

In a core-collapse supernova, an immense burst of neutrinos across all flavors is released, with energies reaching several tens of MeV over a span of seconds. If the supernova occurs close enough, instruments like Super-Kamiokande and Hyper-Kamiokande can detect these neutrinos. Employing similar techniques, effective and efficient measurement of supernova neutrinos has become a priority for future detector designs at ORNL. The precise detection and evaluation of supernova neutrinos can enhance our understanding of supernova physics such as core-collapse mechanisms of massive stars and provide further implications for cosmology and high-energy astrophysics. The Spallation Neutron Source (SNS), managed by the Department of Energy's Office of Basic Energy Sciences, operates around 5,000 hours each year. It delivers 1-GeV proton pulses from a one-microsecond storage ring to a 50 cm thick mercury target at a frequency of 60 Hz. The total luminosity of neutrinos (of any flavor) produced by the SNS during nominal 1-GeV operations at 1.4 MW is about $2.36 \times 10^{15}\ \nu\ s^{-1}$ [1]. ORNL is proposing new detectors with appropriate shielding to mitigate neutron backgrounds from the target.

C. Neutron Backgrounds

Neutrons are produced through various processes in water Cherenkov detectors. The neutrons present in the detector can contribute to background that may interfere with the true neutrino signals. There are four primary interaction types for supernova neutrinos in such detectors: inverse beta decay (IBD, $\overline{\nu_e} + p \rightarrow e^+ + n$), electron elastic scattering (eES, $\nu + e^- \rightarrow \nu + e^-$), charged current interactions on oxygen (^{16}O CC), and neutral current interactions on oxygen (^{16}O NC). The most significant signal in water arises from the inverse beta decay of electron antineutrinos on free protons, which is well understood, along with neutrino-electron scattering [1]. At ORNL, the focus is on detecting and evaluating charged current interactions involving electron neutrinos and ^{16}O, as well as neutral current interactions, all of which are known to be accompanied by neutrons. To accurately interpret the signals from supernova neutrinos and enhance the detector's sensitivity, it is essential to understand the number and spectrum of neutrons emitted during these interactions. Neutrons themselves cannot be directly observed in a water Cherenkov detector at the relevant energies for supernova neutrino detection. Therefore, they must be tagged via the decay products of their captures on materials within the detector. To reduce background, neutron capture techniques and improved shielding can be employed. For our purposes, we will focus on the effects of a shield around the detector made of water and polyethylene, both of which are known to be effective materials for neutron shielding.

II. DETECTOR SETUP

A. Software Used

Geant4[2] was used to build the proposed small water Cherenkov detector and simulate the associated physics and processes. Data analysis and graph generation were subsequently made using ROOT [3] from CERN.

B. Detector Configuration and Geometry

Here, we provide an overview of the geometry and key components of the detector. Fig. 1 presents the view of the detector in Geant4 software.

1. Cylindrical Detector Tank**:** A cylindrical acrylic vessel with a radius of 20 cm and a height of 80 cm, filled with pure water.
2. Sodium Iodide Layer**:** A hollow rectangular shaped Sodium Iodide (NaI) wall around the water vessel.
3. Lead Shielding: A 10.16 cm thick (Pb) rectangular prism shaped shield around the NaI layer.
4. Veto Layer: An outer rectangular prism shaped scintillator layer.
5. Photomultiplier Tubes (PMTs): Fourteen PMTs, each with 3.81 cm (1.5 inches) radius, positioned at the top and bottom face of the vessel. On each face, they are arranged in a hexagonal pattern with one central PMT, spaced 16 cm apart.
6. Neutron Barrier**:** A hollow rectangular prism-shaped barrier with varying thicknesses and a height of 120 cm, made of water or polyethylene, surrounding the entire detector configuration.

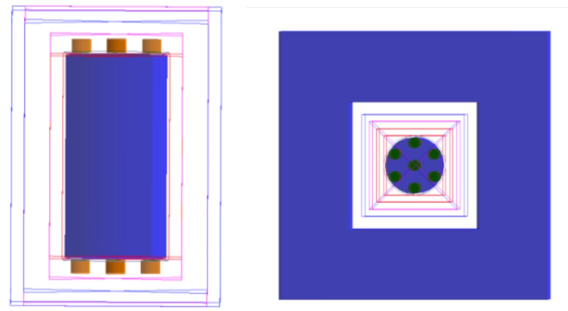

Fig. 1a: Front view of the detector construction in Geant4 without the neutron shield.
Fig. 1b: Top view of the detector construction in Geant4 with the neutron shield.

III. NEUTRON GENERATOR

To study the neutron shielding effects of materials, neutrons are generated from outside the detector. Two different neutron generator models were used for subsequent simulations.

A. Cosmic neutron generator

The cosmic neutron generator is based on Wang's parametrization [4]. It generates a cosmic neutron flux of $17 Hz/m^2$ from a concrete wall surrounding the detector setup. A total of 100,000 events are simulated for various barrier thicknesses. The following formula is used to convert the generated events into an event rate:

$$R = \frac{N_{\text{detected}}}{N_{\text{generated}}} \times \phi \times A$$

In this equation R is the event rate in Hz, N_{detected} is the detected number of events, $N_{\text{generated}}$ *is the* number of generated events, ϕ is the flux in Hz/m^2 ,and A is the surface area over which the particles are generated.

B. Beam Neutron Generator

The beam neutron model is based on an empirical model of the neutron flux in the J-PARC MLF operating at a 300-kW beam [5]. Each "spill" corresponds to one cycle of protons being shot from the accelerator, with the J-PARC MLF operating at a frequency of 25 Hz, meaning 1 spill occurs every 1/25 seconds. For the simulation, 100,000 events were generated, which equates to approximately 258 spills (calculated as 100,000 events divided by 387) at the 300-kW setting. It is important to note that the power at the SNS has recently been increased to 1.7 MW, with plans to further ramp up to 2 MW by summer 2024 [1]. This adjustment was taken into account when calculating the final expected number of events. The model utilizes a single exponential energy spectrum with an isotropic flux generated at the center of the mercury target.

$$\phi(E_n) = \frac{\alpha}{30}\exp\left(-\frac{E_n}{30}\right)$$

Here, normalization factor is α = (387 ± 12)/spills.
In our simulation, neutrons are generated at coordinates $(0, \mathrm{y}, 0)$ with y = 4m.

IV. SIMULATION AND RESULTS

Surrounding the detector, we constructed a hollow rectangular prism-shaped wall with a height of 120 cm and varying thicknesses. The neutron shield is made of either water or polyethylene, and simulations were made for both materials. The thicknesses were set at 50 cm, 100 cm, and increasing up to 300 cm, with neutrons generated outside the detector, using the two generation methods described in the previous section. For each simulation, we recorded the total energy deposited in the water volume and plotted histograms. These plots were generated for each barrier thickness and plotted together on a single figure. Figure 2a shows the results for beam neutrons with a water barrier, while Figure 2b illustrates the results for a polyethylene barrier. Both figures reveal that as the barrier thickness increases, the number of recorded events decreases, indicating that thicker barriers provide more effective neutron shielding. The number of events cross different energy ranges could help determine the reduction rate based on the specific energy of interest. Figure 3 illustrates the total number of recorded events for various barrier thicknesses. As indicated, both water and polyethylene demonstrate comparable shielding performance. For the polyethylene barrier, a thickness of 50 cm achieves a 72% reduction in recorded events, a 100 cm barrier results in an 87% reduction, while a 250 cm barrier is enough for a 99% reduction rate.

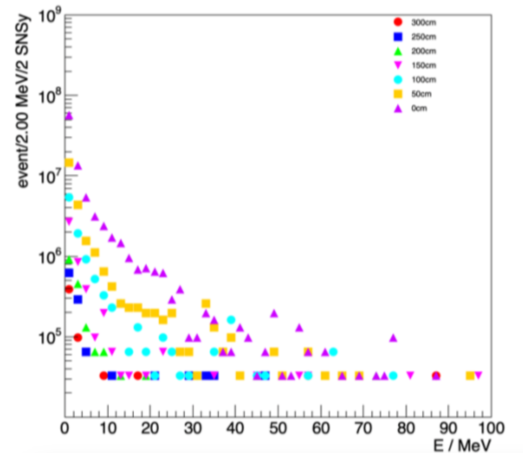

Fig. 2a: Histogram of energy deposition in water Beam neutron generation, water barrier

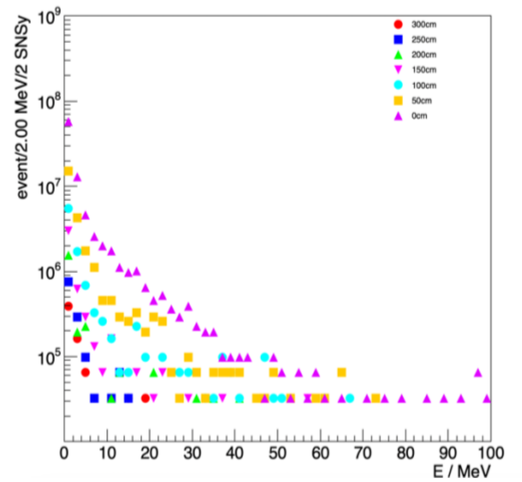

Fig. 2b: Histogram of energy deposition in water Beam neutron generation, polyethylene barrier

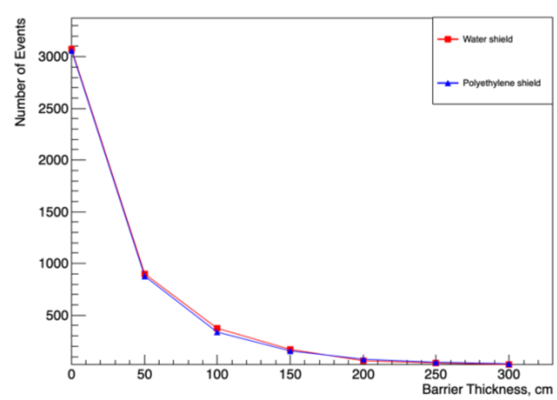

Fig. 3: Plot of number of recorded events for different barrier thicknesses, beam neutrons generated.

Similarly, a histogram of energy deposition in water is generated for the cosmic neutron model. The results indicate that both water and polyethylene barriers exhibit comparable shielding effects. Figure 4a illustrates the total energy deposited in the water volume with a polyethylene barrier. Notably, there is no significant reduction in neutron events as the barrier thickness increases. This observation may be attributed to the barrier's hollow rectangular prism shape, which leaves the top face of the detector exposed and unshielded, allowing neutrons to enter from above, as they are generated in the regions above the barrier.

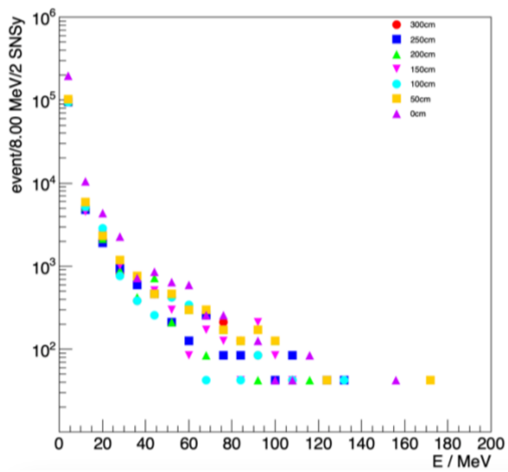

Fig. 4a: Histogram of energy deposition in water Cosmic neutron generation, polyethylene barrier

To address this, an additional layer of rectangular prism polyethylene layer was added on top of the veto surface, measuring 25 cm in height, and matching the inner side length of the original barrier. This modification ensures that the top face of the detector is now covered with polyethylene. Figure 4b presents the results following the addition of the polyethylene layer, which display a significant reduction in neutron events. Furthermore, Figure 5 illustrates the total number of recorded events across various barrier thicknesses. The plot clearly indicates that the inclusion of the extra polyethylene layer contributes to a substantial decrease in neutron events. With a 50 cm barrier, we observe a reduction of 78%, a significant improvement from the original 47% reduction. The 100 cm barrier yields an even greater reduction of 85%. However, there is no significant difference in neutron reduction among the cases with barrier thicknesses greater than 150cm.

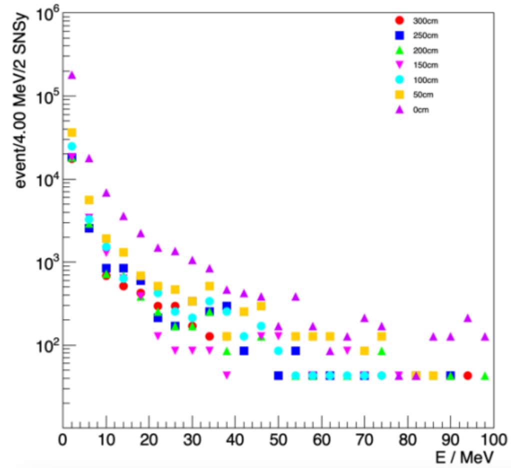

Fig. 4b: Histogram of energy deposition in water Cosmic neutron generation, extra polyethylene layer added.

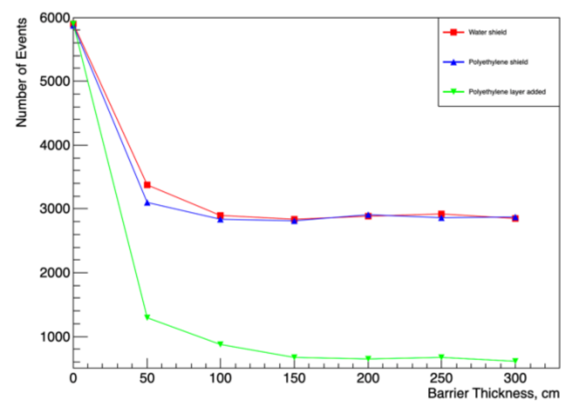

Fig. 5: Plot of number of recorded events for different barrier thicknesses, cosmic neutrons generated.

V. PHOTON COUNTS AND NEUTRON ENERGY RECONSTRUCTION

Optical simulations were conducted to record the number of photons detected by 14 photomultiplier tubes (PMTs). In each simulation, it was observed that the PMTs detect very few photons when the initial neutron energy exceeds 120 MeV, irrespective of the barrier thickness. Furthermore, our findings indicated that the influence of barrier thickness and initial neutron energy on photon counts remains unclear.

Subsequently, an attempt was made to reconstruct the neutron energy signal. Given the challenges in distinguishing between neutron and electron signals in real experimental settings, the reconstruction method assumed that neutron and electron signals are indistinguishable. To reconstruct neutron energy, the research conducted by fellow UTRIP student Ching Yu Leung was referenced. Leung [6] investigated the relationship between electron energy and photon counts. In his simulations, he accelerated electrons of specific energies ranging from 1 MeV to 10 MeV into the water vessel, conducting 100,000 trials to record the average number of hits on photomultiplier tubes (PMTs). The linear relationship identified by Leung under conditions without optical surfaces, can be expressed as follows, where x represents the electron energy in MeV, and y denotes the number of detected photons.

$$y = 26.38x - 14.18$$

With the number of photons recorded, the neutron energy was reconstructed using this conversion and histograms of neutron energy were made. Figure 6a presents the results for the beam neutron generator case, while Figure 6b illustrates the findings for the cosmic neutron case.

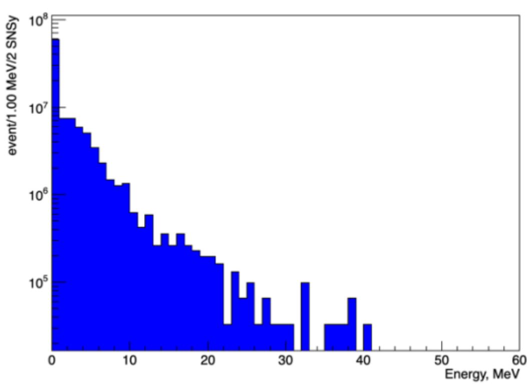

Fig. 6a: Histogram of neutron energy, beam neutron generation

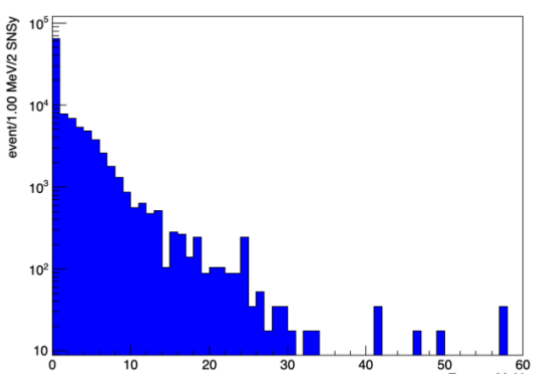

Fig. 6b Histogram of neutron energy, cosmic neutron generation

The plots display neutron energy ranges of 0–60 MeV along with their corresponding frequencies. In a similar manner, neutron energy can be reconstructed for scenarios involving neutron shielding barriers.

VI. CONCLUSIONS

The results demonstrate that both water and polyethylene serve as effective shielding materials for neutron events, showing no significant differences in their performance. The orientation of the shielding layer can be tailored to the specific neutron generation source, while the thickness should be determined based on the desired percentage of events to be shielded. However, optical simulations reveal that the impact of barrier thickness on photon counts remains unclear, with results differing across various energy ranges. Furthermore, there is no strong correlation between initial neutron energy and the number of detected photons. Despite these challenges, the use of optical simulations and the analysis of photon PMT hits hold promise for developing methods to reconstruct neutron signals.

VII. DISCUSSION AND FUTURE WORK

There remains significant potential for further exploration, particularly in testing various neutron barrier configurations and conducting additional simulations. While water and polyethylene are well-known materials for shielding neutrons, experimenting with alternative materials or even combinations of materials could yield valuable insights. In the context of neutron energy reconstruction, a simplistic assumption was made based on the indistinguishability of neutron and electron signals. However, it is important to note that the relationship between photon counts and energy deposition may differ between these two particle types. Obviously, there could be more investigation done for enhancing reconstruction methods and developing more effective approaches for this analysis. Moreover, if time had permitted, running electron simulations on my own detector configuration could have resulted in a more accurate linear relationship for conversion purposes. Finally, a critical question for future investigation is the frequency with which neutrons can be reconstructed within the same energy range as neutrino interactions. From there on, it is essential to quantify the optimal barrier thickness needed to effectively reduce the neutron rate relative to the expected neutrino rate.

ACKNOWLEDGEMENTS

I would like to express my heartfelt gratitude to the UTRIP 2024 organizers and program coordinators for giving me the opportunity to participate in such an enriching program. I am extremely grateful to my research advisor, Professor Nakajima, for his constant support and assistance throughout the program. I would also like to thank my lab members and fellow UTRIP students for their warm welcome and assistance. The interactions I had, the knowledge I gained, and the memories I created during my time in Japan made this experience truly unforgettable, and I am truly grateful to have been a part of it.

REFERENCES

[1] K. Scholberg et al. "White Paper on Neutrino Interaction Measurements for Supernova Neutrino Detection", soon to be published.

[2] "Geant4 Documentation" CERN. (n.d.). https://geant4.web.cern.ch/docs/

[3] "Root reference documentation". CERN. (n.d.). https://root.cern/doc/v632/

[4] Y. F. Wang et al., "Predicting neutron production from cosmic-ray muons" Phys. Rev. D 64, 013012 (2001)

[5] Ajimura et al. "On-site background measurements for the J-PARC E56 experiment: A search for the sterile neutrino at J-Parc MLF" PTEP 2015 6, 063C01 (2015)

[6] Ching Yu Leung "UTRIP research report" (2024)